On the Catalytic Role of the Conserved Active Site Residue His_{466} of Choline Oxidase†

Mahmoud Ghanem‡ and Giovanni Gadda*,‡,§,||

Departments of Chemistry and Biology and The Center for Biotechnology and Drug Design, Georgia State University, Atlanta, Georgia 30302-4098

Received September 9, 2004; Revised Manuscript Received October 8, 2004

ABSTRACT: The oxidation of alcohols to aldehydes is catalyzed by a number of flavin-dependent enzymes, which have been grouped in the glucose-methanol-choline oxidoreductase enzyme superfamily. These enzymes exhibit little sequence similarity in their substrates binding domains, but share a highly conserved catalytic site, suggesting a similar activation mechanism for the oxidation of their substrates. In this study, the fully conserved histidine residue at position 466 of choline oxidase was replaced with an alanine residue by site-directed mutagenesis and the biochemical, spectroscopic, and mechanistic properties of the resulting CHO-H466A mutant enzyme were characterized. CHO-H466A showed k_{cat} and k_{cat}/K_m values with choline as substrate that were 60- and 1000-fold lower than the values for the wild-type enzyme, while the k_{cat}/K_m value for oxygen was unaffected, suggesting the involvement of His_{466} in the oxidation of the alcohol substrate but not in the reduction of oxygen. Replacement of His_{466} with alanine significantly affected the microenvironment of the flavin, as indicated by the altered behavior of CHO-H466A with sulfite and dithionite. In agreement with this conclusion, a midpoint reduction potential of +106 mV for the two-electron transfer in the catalytically competent enzyme−product complex was determined at pH 7 for CHO-H466A, which was ~25 mV more negative than that of the wild-type enzyme. Enzymatic activity in CHO-H466A could be partially rescued with exogenous imidazolium, but not imidazole, consistent with the protonated form of histidine exerting a catalytic role. pH profiles for glycine betaine inhibition, the deprotonation of the N(3)-flavin locus, and the k_{cat}/K_m value for choline all showed a significant shift upward in their pK_a values, consistent with a change in the polarity of the active site. Finally, kinetic isotope effects with isotopically labeled substrate and solvent indicated that the histidine to alanine substitution affected the timing of substrate OH and CH bond cleavages, consistent with removal of the hydroxyl proton being concerted with hydride transfer in the mutant enzyme. All taken together, the results presented in this study suggest that in choline oxidase, His_{466} modulates the electrophilicity of the enzyme-bound flavin and the polarity of the active site, and contributes to the stabilization of the transition state for the oxidation of choline to betaine aldehyde.

The oxidation of alcohols to aldehydes is catalyzed by a number of flavin-dependent enzymes, among which are choline oxidase (*1*, *2*), choline dehydrogenase (*3*), glucose oxidase (*4*, *5*), cholesterol oxidase (*6*), and cellobiose dehydrogenase (*7*). These enzymes all utilize FAD as a cofactor for catalysis and have been grouped in the glucose-methanol-choline (GMC[1]) oxidoreductase enzyme superfamily (*8*). Although GMC enzymes exhibit little sequence similarity in their substrate binding domains, the crystal structures of glucose oxidase (*9*, *10*), cholesterol oxidase (*11*−*13*), and the flavin domain of cellobiose dehydrogenase (*14*) show that they all share a highly conserved catalytic site (Figure 1), suggesting a similar activation mechanism for the oxidation of their substrates. Recent mechanistic studies on choline oxidase with the use of isotopically labeled substrate and solvent indicated that alcohol oxidation occurs through a base-catalyzed formation of an alkoxide species that precedes the transfer of a hydride from the substrate α-carbon to the isoalloxazine system of the FAD cofactor (Scheme 1) (*15*). To date, the nature of both the catalytic base that abstracts the hydroxyl proton from the substrate and the amino acid residue(s) that provide the necessary stabilization of the ensuing alkoxide species in catalysis remains elusive. Earlier mechanistic studies on cholesterol oxidase (*16*, *17*), cellobiose dehydrogenase (*18*), and glucose oxidase (*10*, *19*, *20*), suggested that a histidine residue, which

† This work was supported in part by Grant PRF 37351-G4 from the American Chemical Society and a Research Initiation Grant (G.G.).

* Author to whom correspondence should be addressed: Department of Chemistry, Georgia State University, P.O. Box 4098, Atlanta, GA 30302-4098. Phone: (404) 651-4737. Fax: (404) 651-1416. E-mail: ggadda@gsu.edu.

‡ Department of Chemistry.

§ Department of Biology.

|| The Center for Biotechnology and Drug Design.

[1] Abbreviations: CHO-H466A, mutant form of choline oxidase with His_{466} replaced with Ala; CHO-WT, wild-type choline oxidase; GMC, glucose-methanol-choline oxidoreductase enzyme superfamily; $^{D}k_{cat}/K_m$ and $^{D}k_{cat}/K_{m(D_2O)}$ indicate substrate kinetic isotope effects determined with 1,2-[$^2H_4$]-choline in aqueous and deuterated solvent, respectively; $^{D_2O}k_{cat}/K_m$ and $^{D_2O}k_{cat}/K_{m(D)}$ represent solvent kinetic isotope effects determined with choline and deuterated choline, respectively; $^{D,\,D_2O}k_{cat}/K_m$ is multiple kinetic isotope effect determined with choline in H_2O and deuterated choline in D_2O.

10.1021/bi048056j CCC: $30.25
Published on Web 12/29/2004

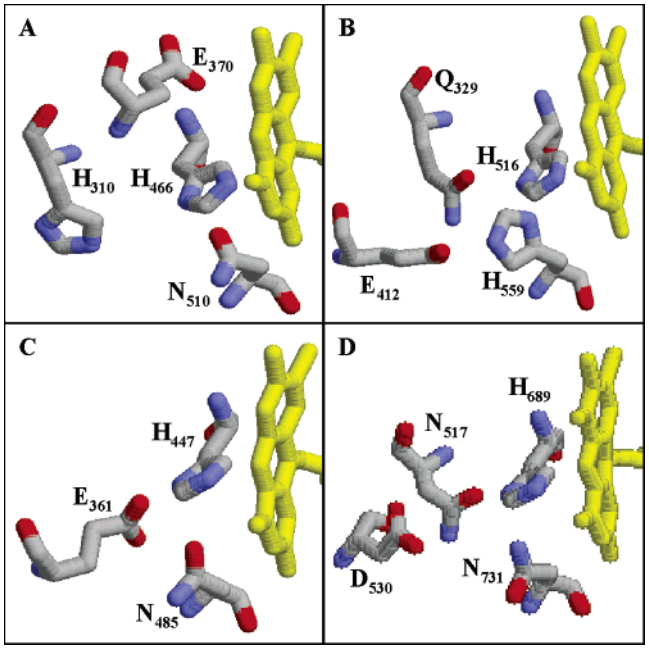

FIGURE 1: The conserved active site residues in the GMC oxidoreductase superfamily. (A) Hypothetical structure of choline oxidase generated by using SWISS-MODEL software and energy minimization by using SYBIL 6.9 software and the structure of glucose oxidase as template. (B) Glucose oxidase (PDB code 1CF3). (C) Cholesterol oxidase (PDB code 1COY). (D) Cellobiose dehydrogenase (PDB code 1NAA).

Scheme 1

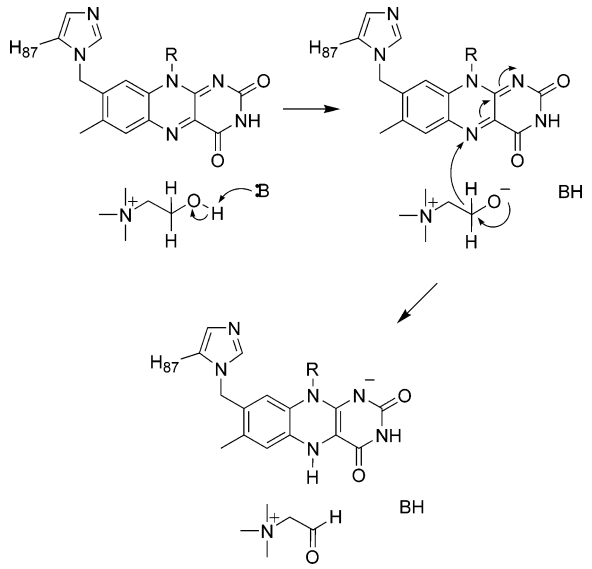

is fully conserved within the GMC family and corresponds to His_{466} of choline oxidase, might act as the specific base that participates in the oxidation of the alcohol substrate (Figure 1). However, the recent availability of a crystal structure of an unliganded form of cholesterol oxidase at subatomic resolution, in which it was shown that the Nϵ2 position of the active site His_{447} residue pointing at the substrate hydroxyl group is protonated (*13*), clearly does not support this histidine residue acting as a specific base in catalysis. These structural observations prompted the authors to suggest that the conserved histidine residue might act as a hydrogen bond donor to the hydroxyl oxygen of the substrate, which would assist in positioning the substrate with respect to the flavin for efficient catalysis (*13*).

Scheme 2

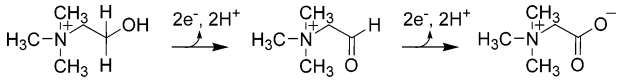

Our group recently cloned and overexpressed the gene coding for choline oxidase (E.C. 1.1.3.17) from *Arthrobacter globiformis* strain ATCC 8010 (*21*), and showed that the resulting enzyme maintains biochemical and kinetic properties similar to those of the native choline oxidase (*21*−*23*). The enzyme is a homodimer of 120 kDa, with each subunit containing covalently bound FAD in an 8α-N(1)-histidyl linkage (*21*, *23*, *24*), and it catalyzes the oxidation of choline to glycine betaine through two sequential flavin-linked hydride transfers from choline and the ensuing betaine aldehyde intermediate to molecular oxygen (Scheme 2) (*15*, *21*−*23*). This reaction is of considerable interest for medical and biotechnological applications, since accumulation of glycine betaine in many pathogens and plants enables their stress resistance toward hyperosmotic environments (*25*, *26*). Consequently, the study of choline oxidase has potential for the development of therapeutic agents that inhibit the biosynthesis of glycine betaine and render pathogenic bacteria susceptible to either conventional treatments or the innate immune system, and for the improvement of water stress resistance in genetically engineered crops lacking efficient glycine betaine biosynthetic systems.

In the present study, a mutant choline oxidase in which the active site residue His_{466} was replaced with alanine was prepared by site-directed mutagenesis, and the biochemical, spectroscopic, and mechanistic properties of the resulting CHO-H466A mutant enzyme were characterized in order to obtain insights on the catalytic role played by this conserved histidine residue. The results of the studies presented herein provide new insights into the chemical mechanism of choline oxidase and, by extension, of the GMC oxidoreductase enzyme superfamily.

EXPERIMENTAL PROCEDURES

Materials. Escherichia coli strain Rosetta(DE3)pLysS was from Novagen (Madison, WI). The QuikChange site-directed mutagenesis kit was from Stratagene (La Jolla, CA). The QIAprep Spin Miniprep kit was from Qiagen (Valencia, CA). Oligonucleotides used for site-directed mutagenesis and for sequencing of the mutant gene were custom synthesized by the DNA Core Facility of the Department of Biology of Georgia State University or by Sigma Genosys (The Woodlands, TX). Oligonucleotides, bovine serum albumin, chloramphenicol, tetracycline, isopropyl-*β*-D-thiogalactopyranoside (IPTG), lysozyme, sodium hydrosulfite (dithionite), sodium sulfite, betaine aldehyde, glycine betaine, Luria−Bertani agar and broth, and PMSF were from Sigma (St. Louis, MO). Choline chloride and ampicillin were from ICN (Aurora, OH). 1,2-[$^2H_4$]-Choline bromide was from Isotec Inc. (Miamisburg, OH). Deuterium oxide (D_2O) was from Cambridge Isotope Laboratories Inc. (Andover, MA). Wild-type choline oxidase (CHO-WT) from *A. globiformis* strain ATCC 8010 was expressed from pET/*codA*1 and purified to homogeneity as previously described (*21*). The fully oxidized FAD-containing CHO-WT was prepared as described in ref *27*. All other reagents were of the highest purity commercially available.

Instruments. UV−visible absorbance spectra were recorded using an Agilent Technologies diode-array spectrophotometer model HP 8453 equipped with a thermostated water bath. Fluorescence emission spectra were recorded with a Shimadzu spectrofluorometer model RF-5301 PC thermostated at 15 °C. Circular dichroism spectra were acquired using a Jasco J-810 spectropolarimeter at 5 °C.

Site-Directed Mutagenesis. A QuikChange kit was used to prepare the mutant enzyme choline oxidase-H466A (CHO-H466A). The method used was essentially according to the manufacturer's instructions, using pET/*codA*1 plasmid (*21*) as a template and Cho-H466Af (5′CAACACCGTCTACGC-CCCCGTGGGCACCGTGC 3′) and Cho-H466Ar (5′CACG-GTGCCCACGGGGGCGTAGACGGTGTTGTGC 3′) oligonucleotides as forward and reverse primers (underlined letters indicate mismatches), respectively. DNA was sequenced at the DNA Core Facility at Georgia State University using an Applied Biosystems Big Dye Kit on an Applied Biosystems model ABI 377 DNA sequencer. Sequencing confirmed the presence of the mutant gene in the correct orientation. *E. coli* strain Rosetta(DE3)pLysS competent cells were transformed with plasmid pET/*codA*1-H466A by electroporation.

Expression and Purification of CHO-H466A. Permanent frozen stocks of *E. coli* cells Rosetta(DE3)pLysS harboring plasmid pET/*codA*1-H466A were used to inoculate 4.5 L of Luria−Bertani broth medium containing 50 μg/mL ampicillin and 34 μg/mL chloramphenicol, and liquid cultures were grown overnight at 37 °C. The cultures were induced for protein expression by adding 0.1 mM IPTG and then incubated for an additional 5 h at 22 °C. A 100 μL aliquot was taken 5 h after induction with IPTG to be used for visualization of the expressed protein using sodium dodecyl sulfate polyacrylamide gel electrophoresis following the Laemmli method (*28*). The gel was stained with Coomassie Brilliant Blue G-250. The mutant enzyme CHO-H466A was purified to homogeneity using the same procedure used previously for the purification of the wild-type enzyme (*21*).

Spectral Studies. The extinction coefficient of CHO-H466A was determined in Tris-Cl, pH 8, after denaturation of the enzyme by treatment with 0.1% SDS at 100 °C for 5 min, based upon the ϵ_{450} value of 11.3 mM^{-1} cm^{-1} for free FAD (*29*). The spectral properties of CHO-WT and CHO-H466A before and after the addition of 200 mM of glycine betaine were determined at 15 °C in 100 mM sodium pyrophosphate buffer, pH 6.5. All spectra were normalized to the molar extinction of the uncomplexed enzyme and corrected for dilution. For reactions with sodium sulfite, the reagent was prepared freshly as 1 M stock solution in 100 mM sodium pyrophosphate, pH 6.5. Different amounts of sodium sulfite at final concentrations ranging from 25 to 100 mM were added to the enzyme solution in 100 mM sodium pyrophosphate, pH 6.5, at 15 °C, and the UV−visible absorbance spectra were recorded at different times. Since previous studies on wild-type choline oxidase showed that the enzyme is reduced by treatment with dithionite in the presence of oxygen (*23*), reduction of CHO-H466A with dithionite was carried out aerobically in 20 mM Tris-Cl, pH 8, at 15 °C, by adding dithionite to the enzyme solution as a powder. The excess amount of dithionite was removed by gel filtration using a Sephadex G-25 column equilibrated with 20 mM Tris-Cl, pH 8. The pH dependence of the absorbance spectra for both wild-type and mutant enzymes at concentrations of ~20 μM in 20 mM sodium phosphate, 20 mM sodium pyrophosphate, pH 6, 15 °C, was determined by titrating with sodium hydroxide.

The CD spectra of CHO-WT and CHO-H466A were recorded at 5 °C in 20 mM Tris-Cl, pH 8, at concentrations of enzyme of 5 and 15 μM for the far and the near UV, respectively. The fluorescence emission spectra of CHO-WT and CHO-H466A were acquired in 20 mM Tris-Cl buffer, pH 8 at 15 °C. The excitation wavelengths for CHO-WT and CHO-H466A were 453 and 458 nm, respectively.

Enzyme Assays. The enzymatic activity of CHO-H466A was measured by the method of initial rates as described for the wild-type enzyme (*21*, *23*) using a computer-interfaced Oxy-32 oxygen-monitoring system (Hansatech Instrument Ltd.). The kinetic parameters of CHO-H466A were determined by varying the concentrations of both choline, in the range between 2.5 and 35 mM, and oxygen, in the range between 24 and 460 μM, as substrates, in 50 mM potassium phosphate, pH 7, at 25 °C. The effect of pH on the kinetic parameters of CHO-H466A was determined over a pH range from 5 to 11 by a series of enzyme activity assays at varying choline concentrations ranging from 0.025 to 45 mM in air-saturated 50 mM sodium pyrophosphate at 25 °C. The kinetic isotope effects of CHO-H466A were obtained by determining the kinetic parameters of the enzyme using either choline or 1,2-[$^2H_4$]-choline as substrate in either aqueous or deuterated solvent, in air-saturated 50 mM sodium pyrophosphate at 25 °C and p*L* 10. For the determinations of solvent isotope effects, buffers were prepared using 99.9% deuterium oxide by adjusting the pD value with NaOD. The pD values were determined by adding 0.4 to the pH electrode readings (*30*). For all steady-state kinetic isotope effects, activity assays were carried out by alternating substrate or solvent isoptomers. Product inhibition studies were carried out by varying the concentrations of both glycine betaine, in the range between zero and 60 mM, and choline, in the range between 0.02 and 20 mM, in air-saturated 50 mM sodium pyrophosphate at 25 °C, over a pH range from 7 to 11. The effect of imidazole on the turnover number of CHO-H466A was determined by measuring the enzymatic activity with 10 mM choline as substrate for the enzyme in the presence of varying concentrations of imidazole in the range from 0 to 250 mM in air-saturated 50 mM potassium phosphate, pH 7, or 50 mM sodium pyrophosphate for other pH values.

Potentiometric Titrations. All redox titrations of wild-type and H466A CHO were carried out on the glycine betaine-liganded enzyme at 15 °C in a cell similar to the one described by Edmondson (1985). Potentials were measured by using a Pt electrode relative to an Ag/AgCl double junction reference electrode with an Orion model 701A pH/mV meter (*31*). The reference electrode was calibrated prior to each titration as described by Edmondson (*31*), using a deoxygenated, saturated quinhydrone solution in 0.09 M KCl and 0.01 M HCl at 25 °C. In a typical titration, 2.5 mL of ~20−30 μM choline oxidase containing glycine betaine at a concentration of 1.5 M in 20 mM Tris-Cl, pH 7, was scrubbed free of oxygen by at least 15 cycles of alternate

degassing under vacuum and flushing with O_2-free argon. The following redox mediators were added to ensure complete redox equilibration: 2 μM methyl viologen (−440 mV), 0.5 μM dichlorophenolindophenol (+217 mV), 0.5 μM phenazine methosulfate (+80mV), 0.5 μM thionin (+60 mV), 0.5 μM duroquinone (−5 to +5 mV), 0.5 μM resorufin (−50 mV), and 0.5 μM indigo carmine (−125 mV) (*32*, *33*). The ligand-bound enzyme solutions were titrated electrochemically as described by Dutton (*34*), using freshly prepared sodium dithionite as reductant and potassium ferricyanide as oxidant in 20 mM Tris-Cl, pH 7 (*34*). Adequate time was permitted for electronic equilibration after each addition of sodium dithionite or potassium ferricyanide prior to the spectrum being recorded; equilibrium of the system was considered to be obtained when the measured potential drift was less than 1 mV in 5 min, which was typically achieved after 30 to 60 min. UV−visible absorbance spectra were recorded using an Agilent Technologies diode-array spectrophotometer model HP 8453 equipped with a thermostated cell holder and a magnetic stirrer beneath the cell holder. All spectra were corrected for any drift in the baseline by subtracting the absorbance at 800 nm.

Data Analysis. Kinetic data were fit with the KaleidaGraph software (Synergy Software, Reading, PA) and the Enzfitter software (Biosoft, Cambridge, U.K.). Apparent kinetic parameters in atmospheric oxygen were determined by fitting initial reaction rates at different substrate concentrations to the Michaelis−Menten equation for one substrate. Initial rates determined by varying the concentration of both choline and oxygen were fit to eq 1, which describes a sequential steady-state kinetic mechanism. K_a and K_b are the Michaelis constants for choline (*A*) and oxygen (*B*), respectively, and k_{cat} is the turnover number of the enzyme (*e*). Data from product inhibition studies were fit to eq 2, which describes the competitive inhibition pattern of the product and the organic substrate. *P* is the concentration of glycine betaine, and K_{is} is the inhibition constant for the slope effect. The pH dependencies of steady-state kinetic parameters were determined by fitting initial rate data to eq 3, which describes a curve with a slope of +1 and a plateau region at high pH. The pH dependence of inhibition by glycine betaine was determined by fitting the initial rate data to eq 4, which describes a curve with a slope of −1 and a plateau region at low pH. *C* is the pH-independent value of the kinetic parameter of interest. Data of the pH dependencies of the absorbance spectra for both wild-type and mutant enzymes were fit to eq 5, which describes a curve with a slope of −1 and plateau regions at low and high pH, where *A* and *B* represent the absorbance values at 500 nm at low and high pH, respectively. The midpoint reduction potentials of the enzymes were determined by fitting the data to the Nernst equation (eq 6), where E_h is the measured electrode potential at equilibrium at each point in the titration; E_m is the midpoint redox potential; *R* is the gas constant, with a value of 8.31 J mol^{-1} at 15 °C; *T* is the temperature in kelvins; *n* is the number of electrons transferred; *F* is Faraday's constant, with a value of 96.48 kJ V^{-1} mol^{-1}.

$$\frac{v}{e} = \frac{k_{cat}AB}{K_aB + K_bA + AB + K_{ia}K_b} \quad (1)$$

$$\frac{v}{e} = \frac{k_{cat}A}{K_a\left(1 + \frac{P}{K_{is}}\right) + A} \quad (2)$$

$$\log Y = \log \frac{C}{1 + \frac{10^{-pH}}{10^{-pK_a}}} \quad (3)$$

$$\log Y = \log \frac{C}{1 + \frac{10^{-pK_a}}{10^{-pH}}} \quad (4)$$

$$Y = \frac{A \times 10^{-pH} + B \times 10^{-pK_a}}{10^{-pH} + 10^{-pK_a}} \quad (5)$$

$$E_h = E_m + \frac{2.303RT}{nF} \log \frac{[FAD_{Ox}]}{[FAD_{Red}]} \quad (6)$$

RESULTS

Expression and Purification of CHO-H466A. CHO-H466A was expressed and purified to homogeneity as judged by SDS−PAGE using the same protocol developed for the wild-type enzyme (data not shown). As for the case of the wild-type enzyme, about 150 mg of pure mutant enzyme could be typically obtained from 4.5 L of Luria−Bertani culture medium. The specific activity of the H466A form of choline oxidase was ∼45 times lower than that of the wild-type enzyme [0.12 vs 5.3 μmol O_2 min^{-1} mg^{-1} (*21*)], suggesting that His_{466} plays a role in catalysis in choline oxidase.

Spectral Properties. In order to verify that the mutant enzyme maintains an overall fold similar to that of the wild-type enzyme, the structural properties of CHO-H466A were examined using CD and fluorescence spectroscopy. The near- and the far-UV CD spectra of CHO-H466A were found to be similar to those of the wild-type enzyme (Figure 2), suggesting an overall fold of the mutant enzyme similar to that of the wild-type enzyme. As shown in Figure 2, the protein fluorescence emission spectrum of CHO-H466A obtained upon excitation at 285 nm yielded a peak at 340 nm, as for the case of the wild-type enzyme, but with increased intensity. Such an increase in fluorescence intensity is consistent with either a decrease in the polarity of the microenvironment surrounding nearby aromatic residues (*35*) or the removal of a quenching effect upon substituting the active site histidine with an alanine residue, both effects attributable to the presence of a tyrosine residue, Tyr_{465}, adjacent to the site of mutation in the amino acid sequence of the enzyme (*21*).

The UV−visible absorbance spectrum of CHO-H466A at pH 8 showed the typical flavin peaks in the near-UV and visible region of the absorbance spectrum (Figure 2), indicating that the enzyme-bound flavin cofactor in the mutant enzyme as purified is in the oxidized state. As expected for an enzyme containing covalently bound FAD, the soluble fraction prepared upon treatment of CHO-H466A with 10% trichloroacetic acid followed by centrifugation to remove the denatured protein was devoid of absorbance (data not shown). A stoichiometry of 0.32 ± 0.05 FAD per monomer of protein was calculated for CHO-H466A,

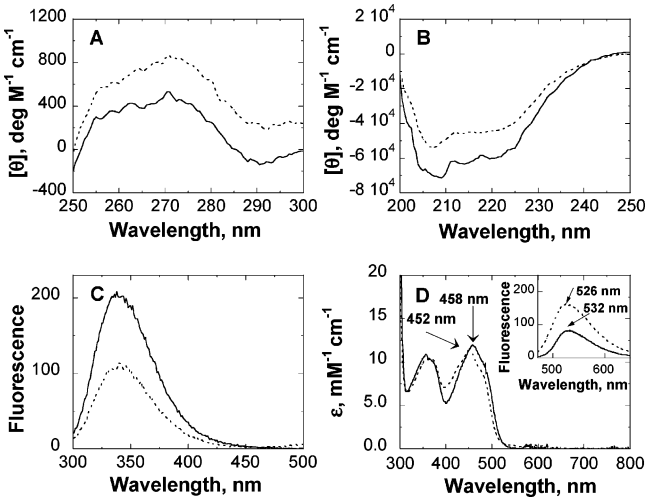

FIGURE 2: Comparison of the spectral properties of CHO-H466A (solid curves) and CHO-WT (dotted curves). (A, B) Circular dichroism spectra of CHO-H466A and CHO-WT in 20 mM Tris-Cl, pH 8, at 5 °C. Enzyme concentrations were 15 and 5 μM for the near-UV and far-UV determinations, respectively. (C) Protein fluorescence emission spectra of CHO-H466A and CHO-WT in 20 mM Tris-Cl, pH 8, at 15 °C; the excitation wavelength was 285 nm for both enzymes. (D) UV−visible absorbance and fluorescence emission spectra of CHO-H466A and CHO-WT in 20 mM Tris-Cl, pH 8, at 15 °C; the excitation wavelengths for CHO-WT and CHO-H466A were 453 and 458 nm, respectively.

indicating that the flavin content of the mutant enzyme was significantly less than that of the wild-type choline oxidase, for which a stoichiometry close to unity was previously reported[2] (*21*). The enzyme-bound flavin of CHO-H466A showed an extinction coefficient at 458 nm of 12 mM^{-1} cm^{-1}, in agreement with the value of 11.4 mM^{-1} cm^{-1} at 452 nm previously determined with the wild-type form of the enzyme (*23*). The flavin fluorescence emission spectrum of CHO-H466A had a maximum at ~530 (λ_{ex} at 458 nm), with a relative intensity of ~50% of that seen for the wild-type enzyme (Figure 2), consistent with an altered flavin microenvironment in the mutant protein.

The absence of a flavin semiquinone in the UV−visible absorbance spectrum of CHO-H466A as purified (Figure 2) is in stark contrast to the observation recently reported for the wild-type form of choline oxidase, for which the enzyme-bound cofactor was found as a mixture of oxidized and air-stable anionic semiquinone flavin species (*21*, *23*). Treatment of the mutant enzyme under aerobic conditions with dithionite at pH 8 resulted in the rapid bleaching of the peak at 458 nm and the appearance of a spectrum with maxima at 372 and 495 nm (data not shown), consistent with reduction of the enzyme-bound flavin to the semiquinone state, as for the case of wild-type enzyme (*23*). However, while no

[2] A lower flavin to protein stoichiometry was reported in earlier studies on mutant forms of trimethylamine dehydrogenase and *p*-cresol methylhydroxylase, in which a positively charged arginine residue in the proximity of the N(1)−C(2)=O locus of the flavin cofactor was selectively replaced (*49*, *55*). Although the low degree of enzyme flavinylation in CHO-H466A was not investigated further in this study, it is reasonable that the low flavin content in the mutated enzyme might be due to the removal of the positively charged His_{466} (vide infra) from the active site of the enzyme, which results in an altered flavin microenvironment in CHO-H466A. In this context, an effect of the alanine replacement of His_{466} on the flavin microenvironment of choline oxidase is supported by several observations presented herein.

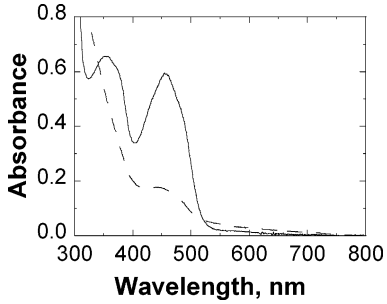

FIGURE 3: Reaction of CHO-H466A with sulfite. UV−visible absorbance spectra of CHO-H466A after 3.5 h of incubation with 100 mM sodium sulfite in the absence (solid curve) or the presence (dashed curve) of 100 mM imidazole. Enzyme concentrations were 50 μM in 100 mM sodium pyrophosphate, pH 6.5, at 15 °C.

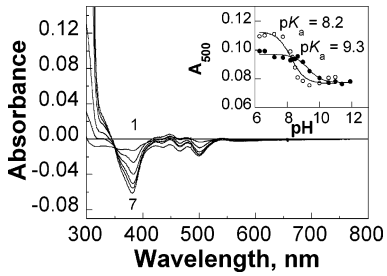

FIGURE 4: Effect of pH on the spectral properties of CHO-H466A and CHO-WT. Absorbance spectra were recorded at an enzyme concentration of 21 μM in 20 mM sodium phosphate, 20 mM sodium pyrophosphate, at 15 °C. Only selected difference absorbance spectra in the pH range between 6 (curve 1) and 12 (curve 7) are shown for CHO-H466A. Inset: UV−visible absorbance values at 500 nm of CHO-H466A (●) and CHO-WT (○) as a function of pH; the curves are fits of the data to eq 5.

spectral changes were observed with the wild-type enzyme upon aerobic incubation at pH 8 of the semiquinone-containing enzyme after removal of the excess dithionite by gel filtration (*23*), complete reoxidation of the enzyme-bound anionic flavin semiquinone was observed with CHO-H466A as indicated by the increase in absorbance at 458 nm (data not shown). These data clearly indicate that the lack of flavin semiquinone in the CHO-H466A protein as purified is due to an impaired ability of this mutant enzyme to stabilize the anionic flavin semiquinone rather than to promote its formation. In contrast to wild-type choline oxidase, which was recently shown to form a tight reversible N(5)-flavin sulfite adduct with a K_d value of ~50 μM at 15 °C (*23*), no significant absorbance changes were observed upon treatment of CHO-H466A with either 25 or 100 mM sodium sulfite at pH 6.5 over 3.5 h of incubation (Figure 3). All taken together, these data further suggest a change in the flavin microenvironment upon replacing His_{466} with alanine.

Effect of pH on the Spectral Properties of CHO-H466A and Wild-Type Choline Oxidase. The effect of pH on the spectral properties of the histidine mutant was determined and compared to that of wild-type enzyme. At pH 6, CHO-H466A exhibited absorbance maxima at 458 and 369 nm, whereas the wild-type enzyme showed maxima at 455 and 357 nm (data not shown). As the pH is increased, a decrease in absorbance in the near-UV and visible regions of the spectra associated with increased resolution in the 430−500 nm region was observed with both CHO-H466A and the wild-type enzymes (Figure 4). Such spectral perturbations are consistent with deprotonation of the FAD at the N(3)-H

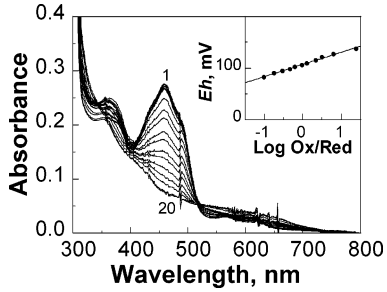

FIGURE 5: Potentiometric redox titration of CHO-H466A in complex with glycine betaine. Curve 1: UV absorbance spectrum of the fully oxidized CHO-H466A at a concentration of ~23 μM in the presence of 1.5 M glycine betaine, in 20 mM Tris-Cl, pH 7, at 15 °C. Curves 2−19: selected intermediate spectra recorded during the reduction of the ligand-bound CHO-H466A after each addition of sodium dithionite. Curve 20: UV absorbance spectrum of the fully reduced ligand-bound CHO-H466A. Inset: Nernst plot of the potentiometric data for the reduction of the enzyme-bound flavin in CHO-H466A. The line is a fit of the data to eq 6.

position occurring as the pH is increased (*36*). From the spectral changes at 500 nm, a pK_a value of 9.3 ± 0.2 was determined for the ionization of the N(3)-H locus of the enzyme-bound 8α-N(1)-histidyl-FAD in CHO-H466A (Figure 4). Such a value compares well with the value of 9.7 that is observed for 8α-*N*-imidazoyl-riboflavin in solution (*31*). In contrast, a pK_a value of 8.2 ± 0.1 was determined for the wild-type enzyme (Figure 4). These data are consistent with His_{466} significantly affecting the ionization of the oxidized flavin at the N(3)-H locus in choline oxidase, and with a change in the flavin microenvironment upon replacing His_{466} with alanine.

Redox Potentiometry. The midpoint reduction−oxidation potential of CHO-H466A in complex with glycine betaine was determined through the reductive titration of the enzyme with sodium dithionite as a reductant, and was compared to that for the wild-type form of the enzyme. This determination was carried out on the glycine betaine−enzyme complex rather than the unliganded enzyme because the catalytic transfers of hydride equivalents from choline and the aldehyde intermediate to molecular oxygen via the flavin cofactor occur when the active site of the enzyme is occupied by either the substrate or the product of the reaction (*22*, *23*). As shown in Figure 5, the oxidized flavin bound to CHO-H466A was reduced to the hydroquinone with no significant formation of semiquinone species, as expected on the basis of previous data indicating that the enzyme under turnover cycles between the oxidized and reduced states[3] (*23*). At pH 7, a midpoint reduction−oxidation potential ($E_{m,7}$) of +106 ± 0.5 mV was determined in two independent experiments for CHO-H466A by fitting the data to the Nernst equation (eq 6). A value of 24 mV was calculated from the slope in a plot of the reduction−oxidation potential as a function of the logarithm of [oxidized]/[reduced] flavin (Figure 5), in good agreement with the theoretical value of 28.5 mV for a two-electron-transfer reaction at 15 °C. A similar analysis of the wild-type enzyme yielded an $E_{m,7}$ value of +132 ± 1 mV for the two-electron transfer in the glycine betaine−enzyme complex (data not shown), a value that is in keeping with previously reported values for other flavoenzymes whose cofactor is covalently linked to the protein, such as *p*-cresol methylhydroxylase ($E_{m,7}$ = 84 mV) (*37*) or vanillyl alcohol oxidase ($E_{m,7}$ = 55 mV) (*38*). Consequently, a ~25 mV decrease in the reduction−oxidation potential of the enzyme-bound flavin is effected by the replacement of the active site histidine with an alanine residue.

Table 1: Steady State Kinetic Parameters of CHO-H466A and CHO-WT with Choline as Substrate at pH 7[a]

kinetic parameters	CHO-H466A	CHO-WT[b]
k_{cat}, s^{-1}	1.1 ± 0.1	61 ± 6
K_a, mM[c]	29 ± 1	1.7 ± 0.3
k_{cat}/K_a, M^{-1} s^{-1} [c]	38 ± 2	36000 ± 6400
K_{O2}, μM	21 ± 2	703 ± 102
k_{cat}/K_{O2}, M^{-1} s^{-1}	55000 ± 5000	87100 ± 15300
K_{ia}, mM	8.5 ± 2.9	0.20 ± 0.05
R^2	0.997	0.998

[a] Enzymatic activity was measured by varying the concentrations of both choline and oxygen in 50 mM potassium phosphate, pH 7, at 25 °C. [b] From ref *23*. [c] K_a and k_{cat}/K_a are the K_m and k_{cat}/K_m values for choline, respectively.

Steady-State Kinetics. The steady-state kinetic parameters for wild-type choline oxidase with choline as substrate were recently reported (*23*). Here, the steady-state kinetic parameters of CHO-H466A were determined by monitoring the rate of oxygen consumption at varying concentrations of both choline and oxygen at pH 7 and 25 °C. As expected from previous data with the wild-type enzyme, the best fit of the data was observed to a sequential steady-state kinetic mechanism (eq 1), consistent with the order of the kinetic steps involving substrate binding and product release being not changed by the substitution of His_{466} with alanine. When the kinetic parameters for CHO-H466A were compared to those of the wild-type enzyme (Table 1), 60- and 1000-fold decreases in the k_{cat} and k_{cat}/K_m values for choline were observed, respectively, indicating a direct participation of His_{466} in the oxidation of choline. In contrast, the k_{cat}/K_m value for oxygen was only 1.5 times lower in CHO-H466A compared to the wild-type enzyme (Table 1), suggesting a minimal involvement of the histidine residue in the oxidation of the enzyme-bound reduced flavin by molecular oxygen.

Rescuing Effects of Imidazole. From a structural standpoint, the histidine to alanine mutation in the active site of choline oxidase is equivalent to the removal of an imidazole moiety from the side chain of the amino acid residue at position 466. In principle, both the kinetic and biochemical properties that have been affected by such a mutation should be at least partially restored in the enzyme in the presence of exogenous imidazole. At pH 7, the k_{cat} value with choline as substrate increased in a concentration-dependent pattern with increasing amounts of exogenous imidazole in the assay reaction mixture (Table 2), indicating that CHO-H466A activity can

[3] Attempts to determine the $E_{m,7}$ through the oxidative titration of the enzyme using potassium ferricyanide as an oxidant failed with both the mutant and wild-type enzymes, mainly due to instability of the enzyme in the reduced state over the prolonged times required for equilibration of the system after each addition of oxidant. Nonetheless, we are confident of the quality of the data reported herein since with both the mutant and wild-type enzymes the $E_{m,7}$ values determined in two independent experiments were in excellent agreement with each other. Furthermore, the $E_{m,7}$ values for both enzymes differed by less than 2% when the data where analyzed by using $A_{458} = [a + b \times 10^{(E_{m,7}-E)/28.5}]/[1 + 10^{(E_{m,7}-E)/28.5})]$, where a and b are component absorbance values contributed by the flavin in the oxidized and reduced states, respectively, and E and $E_{m,7}$ are the electrode potential and the midpoint reduction−oxidation potential for a two-electron transfer process, respectively (*34*, *56*).

Table 2: The Effect of Imidazole on the Turnover Number of CHO-H466A at Different pH Values[a]

pH	k_{cat}, s^{-1} [b]	$k_{cat(imidazole)}$, s^{-1} [b]	$K_{imidazole}$, mM[c]	R^2
5.5	0.03	0.21 ± 0.05	52 ± 6	0.998
6	0.07	0.32 ± 0.02	71 ±15	0.985
7	0.37	0.52 ± 0.06	18 ± 3	0.992
8	0.72	0.67[d]	nd[f]	nd
10	0.73	0.70[e]	nd	nd

[a] Enzymatic activity was measured in the presence of imidazole (0−250 mM) with 10 mM choline as a substrate in 50 mM air-saturated buffer at 25 °C. [b] k_{cat} and $k_{cat(imidazole)}$ are the turnover numbers of the enzyme in the absence and the presence of saturated imidazole, respectively. [c] $K_{imidazole}$ is the concentration of imidazole at which half the maximal turnover number is observed. [d] Turnover number in the presence of 80 mM imidazole. [e] Turnover number in the presence of 100 mM imidazole. [f] Not determined.

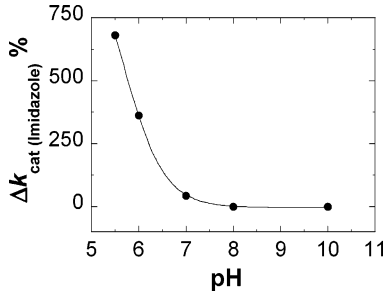

FIGURE 6: pH dependence of the imidazole-rescued activity of CHO-H466A. The percentage of increase in k_{cat} values of CHO-H466A as a function of pH, calculated from the ratio of the k_{cat} value with choline measured in the presence of saturating imidazole to the k_{cat} value measured in the absence of imidazole. The curve is a fit of the data to eq 5.

be rescued by imidazole. In contrast, no significant effect was observed with the wild-type enzyme under the same conditions. Although the effect of imidazole accounted for only a limited rescue of the enzymatic activity of CHO-H466A when compared to that of the wild-type enzyme, i.e., less than 10% at pH 7, it was nonetheless significant and allowed the determination of the effect of pH on the imidazole effect in order to establish whether the protonated or the unprotonated form of imidazole is responsible for the effect. As summarized in Table 2, no changes on k_{cat} with choline were observed in the presence of imidazole at both pH 8 and 10, whereas 5- and 10-fold increases in the k_{cat} values were seen at pH 6 and 5.5, respectively. When the relative increase in the k_{cat} values due to exogenous imidazole was analyzed as a function of pH (Figure 6), the data could be fit to a curve with a slope of −1 (eq 5), indicating a pH effect on the rescuing of the enzymatic activity of CHO-H466A. These results clearly indicate that the protonated form of imidazole is the catalytically relevant species responsible for the partial rescue of enzymatic activity in CHO-H466A, thereby providing strong evidence against His_{466} acting as a the specific base in choline oxidase.

Addition of exogenous imidazole was also effective in restoring the ability of CHO-H466A to stabilize an N(5)-flavin adduct with sulfite, as indicated by the bleaching of the flavin peak at 458 nm upon incubating the enzyme with 100 mM sodium sulfite at pH 6.5 in the presence of 100 mM imidazole (Figure 3).

pH Dependence of the k_{cat} and k_{cat}/K_m Values. Previous pH dependence studies with choline oxidase established the

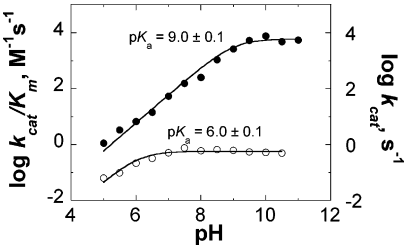

FIGURE 7: pH dependence of k_{cat}/K_m (●) and k_{cat} (○) values of CHO-H466A for choline as substrate. Enzymatic activity was measured at varying concentrations of choline in air-saturated buffer between pH 5 and 11, at 25 °C. The curves are fits of the data to eq 3.

Table 3: Substrate and Solvent Kinetic Isotope Effects on the Oxidation of Choline Catalyzed by CHO-H466A

kinetic parameters	CHO-H466A[a]	CHO-WT[b]
$^{D}k_{cat}/K_m$	6.3 ± 0.8	10.7 ± 2.6
$^{D}k_{cat}/K_{m(D_2O)}$	6.0 ± 0.7	nd[c]
$^{D_2O}k_{cat}/K_m$	2.2 ± 0.3	1.1 ± 0.2
$^{D_2O}k_{cat}/K_{m(D)}$	2.0 ± 0.2	nd
$^{D,D_2O}k_{cat}/K_m$	13.2 ± 1.3	10.4 ± 1.8

[a] Enzymatic activity was measured by varying the concentrations of either choline or 1,2-[$^2H_4$]-choline in air-saturated 50 mM sodium pyrophosphate, p*L* 10, at 25 °C. Values shown are the average of two independent experiments. [b] From ref *15*. [c] Not determined.

requirement of a catalytic base with pK_a value of ∼7.5 in the oxidation of choline but not in the subsequent oxidation of the reduced enzyme-bound flavin (*23*). Here, the kinetic parameters of CHO-H466A were measured as a function of pH by varying the concentration of choline in air-saturated buffer since, as previously shown, with wild-type choline oxidase the pK_a value determined in the k_{cat}/K_m pH profile for the organic substrate is independent of the concentration of oxygen (*15*, *23*, *27*). With CHO-H466A, both the k_{cat}/K_m and k_{cat} values for choline increased with increasing pH and reached limiting values at high pH (Figure 7), consistent with the requirement for an unprotonated group in catalysis with the mutant enzyme. A pK_a value of 9.0 ± 0.1 was determined in the pH profile for the k_{cat}/K_m value, consistent with replacement of the histidine with an alanine at position 466 affecting the electrostatic properties of the active site and with His_{466} not being the active site catalytic base in choline oxidase.[4] A pK_a value of 6.0 ± 0.1 was also determined in the pH profile of the k_{cat} value for CHO-H466A.

Substrate and Solvent Kinetic Isotope Effects. Substrate and solvent kinetic isotope effects on the k_{cat}/K_m value with 1,2-[$^2H_4$]-choline as substrate for wild-type choline oxidase were recently reported and are summarized in Table 3 (*15*). With that enzyme, the observed $^{D}k_{cat}/K_m$ value corresponds to the true kinetic isotope effect and can be used to probe the status of the CH bond in catalysis, since at saturating

[4] In principle, the results of the pH dependence studies of CHO-H466A are also consistent with the histidine residue being the catalytic base in the wild-type enzyme, and with some amino acid residues other than His_{466} becoming the catalytic base in the mutant enzyme devoid of histidine, as originally suggested for H_{447} of cholesterol oxidase (*17*). If this were the case, the increase in the enzymatic activity of the CHO-H466A mutant protein in the presence of imidazole should show pH dependence with maximal effects above pH 7, i.e., above the pK_a value of imidazole, at which the fraction of unprotonated imidazole that might act as a base is higher. The data presented in Figure 6 clearly do not support this alternative interpretation of the pH profile data.

oxygen concentrations both the forward and reverse commitments to catalysis are negligible (*15*). Here, the effect of isotopically substituted choline on the k_{cat}/K_m value with CHO-H466A was determined in air-saturated 50 mM sodium pyrophosphate at pH 10 and 25 °C, at which the true kinetic isotope effects could be measured.[5] With CHO-H466A there was a significant decrease in the $^{D}k_{cat}/K_m$ value with respect to the wild-type enzyme (Table 3), consistent with either a nonlinear transition state in which the stretching vibration of the hydride in motion is not completely lost in the transition state (*39*−*41*), or with the kinetic step in which the substrate CH bond is cleaved becoming partially masked by some other slow kinetic steps in the mutant enzyme. The effect of deuterated solvent, which was previously used to establish that OH bond cleavage of the choline substrate is kinetically fast in the reaction catalyzed by the wild-type enzyme (*15*), was also determined at a p*L* value of 10. As shown in Table 3, a significant $^{D_2O}k_{cat}/K_m$ value was observed with CHO-H466A, suggesting that OH bond cleavage has become partially rate-limiting in the mutant enzyme. No significant changes in the $^{D}k_{cat}/K_m$ value were observed upon substituting H_2O with D_2O. Similarly, the $^{D_2O}k_{cat}/K_m$ value was the same irrespective of the isotopic composition of the substrate. Finally, a multiple kinetic isotope effect on the k_{cat}/K_m value that was equal to the product of the substrate and the solvent isotope effects was determined. These kinetic data are consistent with removal of the hydroxyl proton being concerted with hydride transfer to the flavin in CHO-H466A (*42*). From a mechanistic standpoint, these data indicate that in choline oxidase the replacement of the histidine at position 466 with an alanine residue results in a significant perturbation of the timing of substrate bond cleavage in the oxidation of the choline substrate.

Binding of Glycine Betaine. Recent kinetic data showed that glycine betaine inhibits choline oxidase by binding at the active site of the enzyme, resulting in spectral perturbations of the UV−visible absorbance spectrum (*23*, *27*). Here, the effect of glycine betaine binding on the spectral properties of CHO-H466A was determined and compared to that of the wild-type enzyme by recording the absorbance spectrum for the enzyme before and after the addition of 200 mM glycine betaine, at pH 6.5 and 15 °C. As shown in Figure 8, binding of the inhibitor to the enzyme resulted in significant spectral perturbations in the 300 to 500 nm region of the absorbance spectrum, with a maximal increase in absorbance at ~496 nm. In contrast, the wild-type enzyme produced a maximal increase in absorbance at ~450 nm upon binding glycine betaine (Figure 8). The pH dependence of the inhibition by glycine betaine was determined in atmospheric oxygen using choline as substrate for CHO-H466A. As shown in Figure 8, the data were consistent with a single ionizable group that must be protonated for inhibition, as expected from previous studies on the wild-type enzyme (*23*). Although the pK_a value for such a protonated group was poorly defined due to instability of the CHO-H466A enzyme at high pH values, a pK_a value ≥9 could be estimated from the visual inspection of the data in Figure 8. Such a value is at least 1.5 pH units higher than the value of 7.5 previously determined for wild-type choline oxidase (*23*, *27*, *43*). Interestingly, glycine betaine binding was slightly tighter with CHO-H466A than with the wild-type enzyme, as suggested by the limiting K_{is} values of 5.2 ± 0.5 and 12.5 ± 1.1 determined at low pH for the two enzymes (Figure 8), suggesting that His_{466} does not directly participate in product binding.

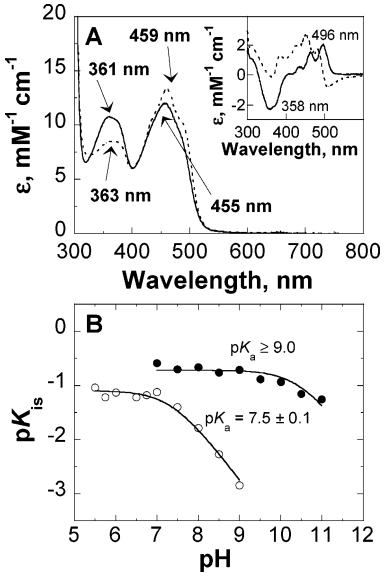

FIGURE 8: Binding of glycine betaine to CHO-H466A. (A) The UV−visible absorbance spectra of CHO-H466A at a concentration of 51 μM were recorded in 100 mM sodium pyrophosphate, pH 6.5 and 15 °C, before (solid curve) and after (dotted curve) the addition of 200 mM glycine betaine. Inset: Comparison of the difference spectrum of CHO-H466A (solid curve) with that of CHO-WT (dotted curve) under the same conditions. (B) Comparison between the pH dependence of the product inhibition of CHO-H466A (●) and wild-type enzyme (○) from ref *23*, using glycine betaine. Enzymatic activity was measured at varying concentrations of choline and glycine betaine in air-saturated buffer between pH 7 and 11 for CHO-H466A, and between pH 5.5 and 9 for wild-type enzyme, at 25 °C. The lines are fits of the data to eq 4. The K_{is} values for glycine betaine were determined by fitting the initial rate data to eq 2.

DISCUSSION

The mutant form of choline oxidase in which the active site histidine at position 466 was replaced by an alanine residue maintains structural and kinetic properties that are similar to those of the wild-type enzyme, as indicated by both the spectroscopic and the steady-state kinetics data presented in this study. Consequently, the mechanistic properties that allow the elucidation of the role this amino acid residue plays in the reaction catalyzed by choline oxidase could be investigated by using a combination of biochemical, spectroscopic, and mechanistic probes.

The active site residue His_{466} is involved in the oxidation of the choline substrate, but not in the following reduction of molecular oxygen catalyzed by choline oxidase. Evidence supporting this conclusion comes from the steady-state kinetic data with CHO-H466A as compared to those with the wild-type enzyme, showing that the k_{cat}/K_m value for choline decreases by 3 orders of magnitude whereas that for

[5] Under atmospheric oxygen conditions at 25 °C (i.e., with a concentration of dissolved oxygen of 0.25 mM), due to the low K_m value for oxygen with a value of 5 ± 2 μM at pH 10 (Ghanem, M., and Gadda, G.; unpublished data), CHO-H466A is >97% saturated with oxygen. Therefore, with CHO-H466A the true kinetic isotope effect could be determined from the $^{D}k_{cat}/K_m$ value under atmospheric conditions.

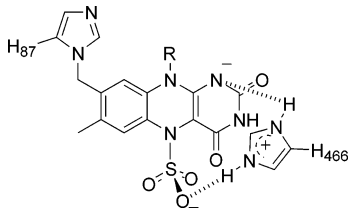

FIGURE 9: Proposed interaction of His_{466} with the flavin N(5)-sulfite adduct.

oxygen is not significantly changed in the mutant enzyme. The lack of involvement of His_{466} in the oxidative half-reaction agrees well with previous kinetic data on choline oxidase as a function of pH, showing that no ionizable groups with pK_a values between 6 and 10 are required for oxidation of the enzyme-bound reduced flavin in catalysis (*23*).

His_{466} is likely not the specific base with pK_a of ~7.5 that abstracts the hydroxyl proton of the substrate in the reductive half-reaction in which choline is oxidized to betaine aldehyde. Strong evidence supporting this conclusion comes from the pH dependence of the imidazole effect with CHO-H466A, showing that imidazolium, but not imidazole, is the catalytically relevant species responsible for the partial rescue of the enzymatic activity of the mutant enzyme. These data are clearly difficult to reconcile with the assumption that His_{466} is the catalytic base participating in the oxidation of choline since, if that were the case, maximal rescue of the enzymatic activity of the mutant enzyme would have been observed at increasing pH. Consistent with His_{466} not being the catalytic base in choline oxidase, the limiting k_{cat}/K_m value with choline at high pH is only ~20-fold lower in CHO-H466A as compared to the wild-type enzyme (*23*). In this respect, recent structural data at subatomic resolution showed that the Nϵ2 atom of the equivalent histidine residue in the active site of cholesterol oxidase, His_{447}, is protonated, suggesting that this conserved residue in the GMC oxidoreductase superfamily may play a role other than acting as a specific base in catalysis (*13*). In this context, a number of observations presented in this study suggest that in choline oxidase His_{466} contributes to catalysis by modulating the electrophilicity of the flavin cofactor and the polarity of the active site, and by stabilizing the negative charge that is formed in the transition state for the oxidation of choline to betaine aldehyde.

A significant contribution to the electrophilicity of the FAD cofactor, which accounts for a fraction of the decreased rate of choline oxidation, is provided by the side chain of His_{466}, as indicated by the decrease of ~25 mV in the midpoint reduction potential of the enzyme-bound flavin in CHO-H466A with respect to the wild-type choline oxidase. A direct electrostatic interaction of the imidazole side chain, through its Nϵ2 locus, and the N(1) locus of the flavin cofactor was previously proposed in glucose oxidase on the basis of X-ray crystallographic data (*9*), suggesting that an analogous interaction might occur in choline oxidase (Figure 9). Evidence supporting the presence of such an interaction in choline oxidase is provided by the lack of stabilization of the anionic flavin semiquinone and of the sulfite N(5)-flavin adduct that were observed with CHO-H466A, which is consistent with a change in the protein microenvironment surrounding the N(1)−C(2)═O region of the flavin (*44*−*50*). From the $\Delta E_{m,7}$ value of −25 mV determined upon replacing H_{466} with alanine in choline oxidase one can calculate an energetic contribution of ~4.2 kJ mol^{-1}, which accounts for a 5-fold decrease in the rate of hydride transfer to the flavin in the mutant enzyme as compared to the wild-type form of choline oxidase. Since mechanistic investigations on wild-type choline oxidase are consistent with the k_{cat}/K_m value for choline reflecting the kinetic step of choline oxidation (*15*), a ~20-fold decrease in the rate of choline oxidation can be estimated from the ratio of the limiting k_{cat}/K_m values for choline at high pH determined in this study with CHO-H466A and the wild-type enzyme (*23*). Consequently, while His_{466} contributes to the electrophilicity of the enzyme-bound flavin for efficient substrate oxidation, such an effect cannot fully explain the decreased catalytic activity observed with the mutant enzyme, consistent with His_{466} contributing to catalysis by using also other strategies (vide infra). The modulation of the redox potential of the flavin does not appear to correlate with the rate of electron transfer from the reduced flavin to molecular oxygen, as indicated by the similar k_{cat}/K_m values for oxygen of CHO-H466A and the wild-type enzyme. Thus, it is likely that other factors, such as steric or solvation effects, are important in the activation of the reduced flavin for reaction with molecular oxygen.

His_{466} provides stabilization to the transition state that is formed in the oxidation of choline to betaine aldehyde, thereby facilitating the activation of the alcohol substrate for facile hydride transfer to the flavin cofactor (Scheme 3). Such a transition state in the mechanism of choline oxidase is supported by mechanistic studies on the wild-type form of choline oxidase using substrate and solvent deuterium kinetic isotope effects (*15*). Evidence for stabilization of the alkoxide species by His_{466} comes from the effects of histidine replacement on the relative timing for bond cleavage in the mutant enzyme, showing that the hydroxyl proton is in flight in the transition state for CH bond cleavage. Indeed, the loss of stabilization of the alkoxide species would make its formation energetically unfavorable, resulting in the loss of the "chelating effect" provided by the electrostatic interaction in the wild-type enzyme. In the absence of such a "chelating effect" catalysis would still occur, but it would be significantly slower because it requires that the vibrational motions of the pairs of atoms involved in bond breaking and making, i.e., the hydroxyl proton and the catalytic base along with the flavin N(5) and the α-carbon hydrogen, be in phase to allow both proton and hydride transfer to occur. Alternatively, initiation of the hydride transfer would decrease the pK_a of the oxygen sufficiently for proton transfer to the catalytic base. In either case, removal of the hydroxyl proton would be concerted with hydride transfer, as was observed with CHO-H466A. Independent evidence for stabilization of the alkoxide species comes from the complete loss of the ability of CHO-H466A to form an N(5)-flavin adduct with sulfite, which is restored in the presence of exogenous imidazole. Although following the seminal work of Massey (*46*−*48*) the ability of flavoenzymes to stabilize a tight flavin adduct with sulfite has been mainly used as a probe of the electrophilicity of the flavin, N(5)-flavin adducts with sulfite depend also on steric factors as well as stabilizing interactions in the active site. With choline oxidase, it is likely that the negatively charged oxygen atom of the sulfite N(5)-flavin adduct is stabilized by a direct interaction with the side chain

Scheme 3

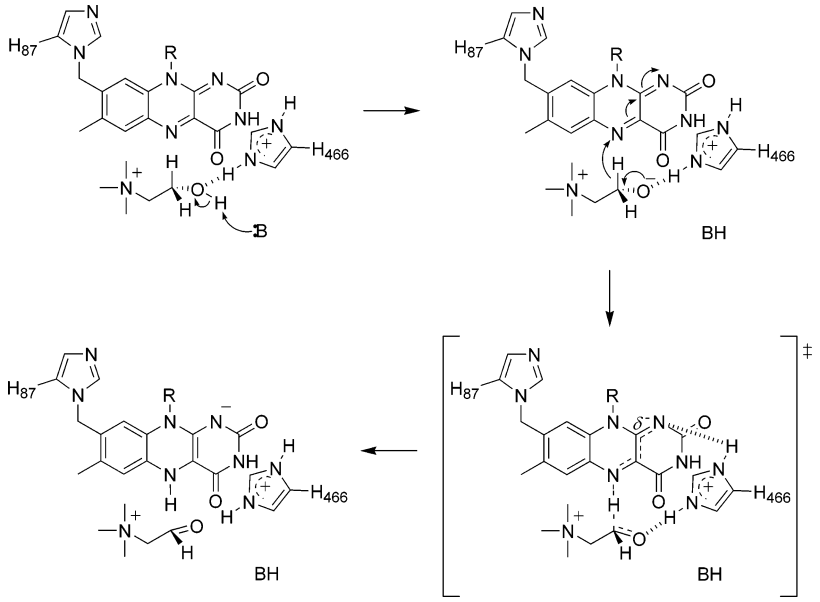

of His_{466} (Figure 9). In the absence of this interaction, such as in the case of CHO-H466A, the N(5)-flavin adduct with sulfite would not be stabilized; exogenous imidazole would restore such an interaction in the mutant enzyme by bridging the methyl side chain of the alanine residue at position 466 to the oxygen atom of the sulfite−flavin adduct. Such a direct interaction between the sulfite oxygen and an active site amino acid residue was previously observed in the three-dimensional structures of flavocytochrome b_2 (*51*) and glycolate oxidase (*50*), providing direct structural support for an analogous interaction in choline oxidase. The stabilization of the transition state is likely provided by the protonated form of His_{466}, as suggested by the pH studies on the rescuing effect of the activity of CHO-H466A by exogenous imidazole, showing that the enzymatic activity of the mutant enzyme can be partially restored by imidazolium, but not imidazole. A stabilization of an alkoxide species by an active site tyrosine residue similar to that proposed here for His_{466} of choline oxidase was recently proposed in flavocytochrome b_2 (*52*), suggesting that this might be a common strategy utilized by flavin-dependent enzymes for the oxidation of inactivated as well as activated alcohols, such as α-hydroxy acids.

The polarity of the active site, which is essential for efficient proton transfer of the hydroxyl proton from the alcohol substrate to the active site proton acceptor, is modulated by His_{466}. Evidence supporting this conclusion comes from the pH profiles of the absorbance spectra of CHO-H466A and the wild-type enzyme, showing that the pK_a value for the ionization of the N(3) locus of FAD increases by one pH unit upon substituting His_{466} with alanine. Such an increase in the pK_a value is consistent with a decreased polarity in the protein microenvironment surrounding the flavin N(3) locus (*36*). Consistent with a less polar active site, an increase in both the protein fluorescence of the unliganded enzyme and the absorbance at 496 nm of the enzyme in complex with glycine betaine is seen with CHO-H466A with respect to the wild-type enzyme (*35*, *36*). The decrease in polarity of the active site of CHO-H466A results in the perturbation of equilibria for ionization of groups that participate in catalysis, among which is the amino acid group that accepts the hydroxyl proton from the substrate. Indeed, in CHO-H466A the pK_a value for the catalytic base in the active site is raised from 7.5 to ∼9, as indicated by the pH profile of the k_{cat}/K_m values for choline. In agreement with previous studies on wild-type choline oxidase (*23*), the same pK_a value of ∼9 is seen in the pH-profile of glycine betaine inhibition with CHO-H466A. Thus, His_{466} appears to be important for regulating the reactivity of the catalytic base that accepts the hydroxyl proton of the substrate for efficient catalysis.

On the basis of the results of the rescuing experiments with imidazole, showing that the activity of CHO-H466A can be partially rescued by imidazolium, one would expect His_{466} to interact with the carboxylate moiety of the glycine betaine product of the reaction. This expectation would be reinforced by the proposed role for His_{466} in the stabilization of the alkoxide intermediate, since both the alkoxide and the carboxylate bear negatively charged oxygen. If this were the case, a significant increase to the extent of 2 to 3 orders of magnitude should be observed in the inhibition constant for glycine betaine with the CHO-H466A enzyme, as in the case of mutant forms of D-amino acid oxidase (*45*) or sarcosine oxidase (*53*), where positively charged groups on the enzyme that ion pair the carboxylate moieties of the product were replaced. However, the results of the product inhibition studies show that binding of glycine betaine to CHO-H466A is unaffected, if not slightly tighter, with respect to the wild-type enzyme. In this respect, recent studies with a number of substituted product analogues indicated that in choline oxidase the acetate moiety of glycine betaine does not contribute to binding, but that the trimethylammonium headgroup is a major determinant instead (*27*). This apparent discrepancy of His_{466} interacting with the negatively charged oxygen of the transient alkoxide species but not with that of the carboxylate product is readily dissipated when one considers the spatial location of their respective oxygen atoms with respect to the histidine residue. Indeed, while the positioning of both the alkoxide and the product is dictated by the interactions established in the active site by the

trimethylammonium headgroup (*27*), the alkoxide oxygen is linked to an sp^3-hybridized carbon whereas the carboxylate oxygen is attached to an sp^2-hybridized carbon. The change from the tetrahedral configuration of the alkoxide to the planar configuration of the carboxylate-containing product results in the carboxylate oxygen moving ~1 Å away from the side chain of His_{466}, thereby abating the electrostatic interaction between the two charges. Although the results presented here do not allow us to draw any conclusion concerning the binding of the substrate in choline oxidase, it is expected that, due to the lack of a negatively charged oxygen, binding of choline is somewhat weaker than that of the alkoxide. A similar result where substitution of an active site histidine residue resulted in differential binding of the substrate and the transition state was recently reported for (*S*)-mandelate dehydrogenase (*54*).

In summary, the results presented herein using a combination of biochemical, spectroscopic, and mechanistic approaches support evidence for the conserved His_{466} playing multiple, but equally important, roles in the oxidation of the alcohol substrate catalyzed by choline oxidase. This residue modulates the electrophilicity of the enzyme-bound FAD for efficient hydride transfer from the substrate; it contributes to the polarity of the active site for efficient proton transfer from the substrate hydroxyl oxygen; and, it stabilizes the choline alkoxide transient species to facilitate hydride transfer from the substrate to the flavin. In light of the structural similarities among the members of the GMC oxidoreductase superfamily, the present results strongly suggest that those enzymes that catalyze the oxidation of unpolarized alcohols are likely to use similar catalytic strategies. Finally, the conclusions presented herein provide an example of the difficulty in developing a comprehensive description of the role carried out by amino acid residues located at the active site of enzymes, which arises from the complex nature of enzyme function to which individual residues are likely to contribute through multiple strategies. Current studies in our laboratory are aimed at the elucidation of the nature of the catalytic base that abstracts the hydroxyl proton from the alcohol substrate in the active site of choline oxidase.

ACKNOWLEDGMENT

The authors thank Dr. Dale E. Edmondson at the Department of Biochemistry of Emory University, Atlanta, for his assistance and guidance in the determination of the redox potentials using the potentiometric method, and Fan Fan for building the hypothetical three-dimensional model of choline oxidase and her assistance in the preparation of Figure 1. The authors also thank Dr. Thomas L. Netzel for discussions on the "chelating effect" in catalysis by choline oxidase.

REFERENCES

1. Ohishi, N., and Yagi, K. (1979) Covalently bound flavin as prosthetic group of choline oxidase, *Biochem. Biophys. Res. Commun. 86*, 1084−8.
2. Ikuta, S., Imamura, S., Misaki, H., and Horiuti, Y. (1977) Purification and characterization of choline oxidase from *Arthrobacter globiformis*, *J. Biochem. (Tokyo) 82*, 1741−9.
3. Tsuge, H., Nakano, Y., Onishi, H., Futamura, Y., and Ohashi, K. (1980) A novel purification and some properties of rat liver mitochondrial choline dehydrogenase, *Biochim. Biophys. Acta 614*, 274−84.
4. Weibel, M. K., and Bright, H. J. (1971) The glucose oxidase mechanism. Interpretation of the pH dependence, *J. Biol. Chem. 246*, 2734−44.
5. Gibson, Q. H., Swoboda, B. E., and Massey, V. (1964) Kinetics and Mechanism of Action of Glucose Oxidase, *J. Biol. Chem. 239*, 3927−34.
6. Kamei, T., Takiguchi, Y., Suzuki, H., Matsuzaki, M., and Nakamura, S. (1978) Purification of 3β-hydroxysteroid oxidase of *Streptomyces violascens* origin by affinity chromatography on cholesterol, *Chem. Pharm. Bull. (Tokyo) 26*, 2799−804.
7. Higham, C. W., Gordon-Smith, D., Dempsey, C. E., and Wood, P. M. (1994) Direct 1H NMR evidence for conversion of β-D-cellobiose to cellobionolactone by cellobiose dehydrogenase from *Phanerochaete chrysosporium*, *FEBS Lett. 351*, 128−32.
8. Cavener, D. R. (1992) GMC oxidoreductases. A newly defined family of homologous proteins with diverse catalytic activities, *J. Mol. Biol. 223*, 811−4.
9. Hecht, H. J., Kalisz, H. M., Hendle, J., Schmid, R. D., Schomburg, D. (1993) Crystal structure of glucose oxidase from *Aspergillus niger* refined at 2.3 Å resolution, *J. Mol. Biol. 229*, 153−72.
10. Wohlfahrt, G., Witt, S., Hendle, J., Schomburg, D., Kalisz, H. M., and Hecht, H. J. (1999) 1.8 and 1.9 Å resolution structures of the *Penicillium amagasakiense* and *Aspergillus niger* glucose oxidases as a basis for modeling substrate complexes, *Acta Crystallogr., Sect. D: Biol. Crystallogr. 55*, 969−77.
11. Vrielink, A., Lloyd, L. F., and Blow, D. M. (1991) Crystal structure of cholesterol oxidase from *Brevibacterium sterolicum* refined at 1.8 Å resolution, *J. Mol. Biol. 219*, 533−54.
12. Li, J., Vrielink, A., Brick, P., and Blow, D. M. (1993) Crystal structure of cholesterol oxidase complexed with a steroid substrate: implications for flavin adenine dinucleotide dependent alcohol oxidases, *Biochemistry 32*, 11507−15.
13. Lario, P. I., Sampson, N., and Vrielink, A. (2003) Sub-atomic resolution crystal structure of cholesterol oxidase: what atomic resolution crystallography reveals about enzyme mechanism and the role of the FAD cofactor in redox activity, *J. Mol. Biol. 326*, 1635−50.
14. Hallberg, B. M., Henriksson, G., Pettersson, G., and Divne, C. (2002) Crystal structure of the flavoprotein domain of the extracellular flavocytochrome cellobiose dehydrogenase, *J. Mol. Biol. 315*, 421−34.
15. Fan, F., and Gadda, G. (2005) On the catalytic mechanism of choline oxidase, *J. Am. Chem. Soc.*, in press.
16. Yin, Y., Liu, P., Anderson, R. G., and Sampson, N. S. (2002) Construction of a catalytically inactive cholesterol oxidase mutant: investigation of the interplay between active site-residues glutamate 361 and histidine 447, *Arch. Biochem. Biophys. 402*, 235−42.
17. Kass, I. J., and Sampson, N. S. (1998) Evaluation of the role of His447 in the reaction catalyzed by cholesterol oxidase, *Biochemistry 37*, 17990-8000.
18. Rotsaert, F. A., Renganathan, V., and Gold, M. H. (2003) Role of the flavin domain residues, His689 and Asn732, in the catalytic mechanism of cellobiose dehydrogenase from *Phanerochaete chrysosporium*, *Biochemistry 42*, 4049−56.
19. Su, Q., and Klinman, J. P. (1999) Nature of oxygen activation in glucose oxidase from *Aspergillus niger*: the importance of electrostatic stabilization in superoxide formation, *Biochemistry 38*, 8572−81.
20. Roth, J. P., and Klinman, J. P. (2003) Catalysis of electron transfer during activation of O_2 by the flavoprotein glucose oxidase, *Proc. Natl. Acad. Sci. U.S.A. 100*, 62−7.
21. Fan, F., Ghanem, M., and Gadda, G. (2004) Cloning, sequence analysis, and purification of choline oxidase from *Arthrobacter globiformis*: a bacterial enzyme involved in osmotic stress tolerance, *Arch. Biochem. Biophys. 421*, 149−58.
22. Gadda, G. (2003) Kinetic mechanism of choline oxidase from *Arthrobacter globiformis*, *Biochim. Biophys. Acta 1646*, 112−8.
23. Ghanem, M., Fan, F., Francis, K., and Gadda, G. (2003) Spectroscopic and kinetic properties of recombinant choline oxidase from *Arthrobacter globiformis*, *Biochemistry 42*, 15179−88.
24. Rand, T., Halkier, T., and Hansen, O. C. (2003) Structural characterization and mapping of the covalently linked FAD cofactor in choline oxidase from *Arthrobacter globiformis*, *Biochemistry 42*, 7188−94.
25. Burg, M. B., Kwon, E. D., and Kultz, D. (1997) Regulation of gene expression by hypertonicity, *Annu. Rev. Physiol. 59*, 437−55.

26. McNeil, S. D., Nuccio, M. L., and Hanson, A. D. (1999) Betaines and related osmoprotectants. Targets for metabolic engineering of stress resistance, *Plant Physiol. 120*, 945−50.
27. Gadda, G., Powell, N., and Menon, P. (2004) The trimethyammonium headgroup of choline is a major determinant for substrate binding and specificity in choline oxidase, *Arch. Biochem. Biophys. 430*, 264−73.
28. Laemmli, U. K. (1970) Cleavage of structural proteins during the assembly of the head of bacteriophage T4, *Nature 227*, 680−5.
29. Whitby, L. G. (1953) A new method for preparing flavin-adenine dinucleotide, *Biochem. J. 54*, 437−42.
30. Schowen, K. B., and Schowen, R. L. (1982) Solvent isotope effects of enzyme systems, *Methods Enzymol. 87*, 551−606.
31. Williamson, G., and Edmondson, D. E. (1985) Effect of pH on oxidation-reduction potentials of 8 α-N-imidazole-substituted flavins, *Biochemistry 24*, 7790−7.
32. Ma, Y. C., Funk, M., Dunham, W. R., and Komuniecki, R. (1993) Purification and characterization of electron-transfer flavoprotein: rhodoquinone oxidoreductase from anaerobic mitochondria of the adult parasitic nematode, *Ascaris suum*, *J. Biol. Chem. 268*, 20360−5.
33. Mohsen, A. W., Rigby, S. E., Jensen, K. F., Munro, A. W., and Scrutton, N. S. (2004) Thermodynamic Basis of Electron Transfer in Dihydroorotate Dehydrogenase B from *Lactococcus lactis*: Analysis by Potentiometry, EPR Spectroscopy, and ENDOR Spectroscopy, *Biochemistry 43*, 6498−510.
34. Dutton, P. L. (1978) Redox potentiometry: determination of midpoint potentials of oxidation-reduction components of biological electron-transfer systems, *Methods Enzymol. 54*, 411−35.
35. Nakajou, K., Watanabe, H., Kragh-Hansen, U., Maruyama, T., and Otagiri, M. (2003) The effect of glycation on the structure, function and biological fate of human serum albumin as revealed by recombinant mutants, *Biochim. Biophys. Acta 1623*, 88−97.
36. Massey, V., and Ganther, H. (1965) On the interpretation of the absorption spectra of flavoproteins with special reference to D-amino acid oxidase, *Biochemistry 4*, 1161−73.
37. Efimov, I., Cronin, C. N., and McIntire, W. S. (2001) Effects of noncovalent and covalent FAD binding on the redox and catalytic properties of *p*-cresol methylhydroxylase, *Biochemistry 40*, 2155−66.
38. Fraaije, M. W., van den Heuvel, R. H., van Berkel, W. J., and Mattevi, A. (1999) Covalent flavinylation is essential for efficient redox catalysis in vanillyl-alcohol oxidase, *J. Biol. Chem. 274*, 35514−20.
39. Winstein, S., and Takahashi, J. (1958) Neighboring hydrogen, isotope effect, and conformation in solvolysis of 3-methyl-2-butyl *p*-toluenesulfonate, *Tetrahedron 2*, 316−21.
40. Collins, C. J., Rainey, W. T., Smith, W. B., and Kaye, I. A. (1959) Molecular Rearrangements. XIV. The Hydrogen−Deuterium Isotope Effect in the Pinacol Rearrangement of Triarylethylene Glycols, *J. Am. Chem. Soc. 81*, 460−6.
41. Hawthorne, M. F., and Lewis, E. S. (1958) Amine Boranes. III. Hydrolysis of Pyridine Diphenylborane and the Mechanism of Hydride Transfer Reactions, *J. Am. Chem. Soc. 80*, 4296−9.
42. Cleland, W. W. (1991) in *Enzyme mechanism from isotope effects* (Cook, P. F., Ed.) pp 291−311, CRC Press, Boca Raton, FL.
43. Gadda, G. (2003) pH and deuterium kinetic isotope effects studies on the oxidation of choline to betaine-aldehyde catalyzed by choline oxidase, *Biochim. Biophys. Acta 1650*, 4−9.
44. Müh, U., Williams, C. H., Jr., and Massey, V. (1994) Lactate monooxygenase. II. Site-directed mutagenesis of the postulated active site base histidine 290, *J. Biol. Chem. 269*, 7989−93.
45. Molla, G., Porrini, D., Job, V., Motteran, L., Vegezzi, C., Campaner, S., Pilone, M. S., and Pollegioni, L. (2000) Role of arginine 285 in the active site of *Rhodotorula gracilis* D-amino acid oxidase. A site-directed mutagenesis study, *J. Biol. Chem. 275*, 24715−21.
46. Müller, F., and Massey, V. (1969) Flavin-sulfite complexes and their structures, *J. Biol. Chem. 244*, 4007−16.
47. Massey, V., Müller, F., Feldberg, R., Schuman, M., Sullivan, P. A., Howell, L. G., Mayhew, S. G., Matthews, R. G., and Foust, G. P. (1969) The reactivity of flavoproteins with sulfite. Possible relevance to the problem of oxygen reactivity, *J. Biol. Chem. 244*, 3999−4006.
48. Massey, V., and Hemmerich, P. (1980) Active-site probes of flavoproteins, *Biochem. Soc. Trans. 8*, 246−57.
49. Efimov, I., Cronin, C. N., Bergmann, D. J., Kuusk, V., and McIntire, W. S. (2004) Insight into covalent flavinylation and catalysis from redox, spectral, and kinetic analyses of the R474K mutant of the flavoprotein subunit of *p*-cresol methylhydroxylase, *Biochemistry 43*, 6138−48.
50. Stenberg, K., Clausen, T., Lindqvist, Y., and Macheroux, P. (1995) Involvement of Tyr24 and Trp108 in substrate binding and substrate specificity of glycolate oxidase, *Eur. J. Biochem. 228*, 408−16.
51. Tegoni, M., and Cambillau, C. (1994) Structural studies on recombinant and point mutants of flavocytochrome *b*2, *Biochimie 76*, 501−14.
52. Sobrado, P., and Fitzpatrick, P. F. (2003) Solvent and primary deuterium isotope effects show that lactate CH and OH bond cleavages are concerted in Y254F flavocytochrome *b*2, consistent with a hydride transfer mechanism, *Biochemistry 42*, 15208−14.
53. Zhao, G., Song, H., Chen, Z. W., Mathews, F. S., and Jorns, M. S. (2002) Monomeric sarcosine oxidase: role of histidine 269 in catalysis, *Biochemistry 41*, 9751−64.
54. Lehoux, I. E., and Mitra, B. (2000) Role of arginine 277 in (*S*)-mandelate dehydrogenase from *Pseudomonas putida* in substrate binding and transition state stabilization, *Biochemistry 39*, 10055−65.
55. Mewies, M., Packman, L. C., Mathews, F. S., and Scrutton, N. S. (1996) Flavinylation in wild-type trimethylamine dehydrogenase and differentially charged mutant enzymes: a study of the protein environment around the N1 of the flavin isoalloxazine, *Biochem. J. 317*, 267−72.
56. Daff, S. N., Chapman, S. K., Turner, K. L., Holt, R. A., Govindaraj, S., Poulos, T. L., and Munro, A. W. (1997) Redox control of the catalytic cycle of flavocytochrome P-450 BM3, *Biochemistry 36*, 13816−23.

BI048056J